Multiple Finger Expansion for Blind Interference Canceller in the Presence of Subchip-Spaced Multipath Components

Tony Q. S. Quek, Hiroshi Suzuki, and Kazuhiko Fukawa

Abstract: **A blind interference canceller in the presence of subchip-spaced multipath channels for direct-sequence code division multiple access (DS-CDMA) down-link system is considered. This technique is based on combining the existing blind interference canceller with a technique that involves assigning subchip-tap spacing to the Rake receiver. The proposed receiver minimizes the receiver's output energy subject to a constraint in order to mitigate the multiple access interference (MAI) along each multipath component, and then suboptimally combining all the multipath components. Moreover, it is able to mitigate the mismatch problem when subchip-spaced multipath components arrive at the blind interference canceller. It is known that optimal combining techniques perform a decorrelation operation before combining, which requires both knowledge and computational complexity. In the following, we have adopted a simpler but suboptimum approach in the combining of the suppressed signals at the output of our proposed receiver. Computer simulation results verify the effectiveness of the proposed receiver to handle subchip-spaced multipath components and still suppresses MAI significantly.**

Index Terms: **Blind interference canceller, rake, MAI, mismatch problem, subchip-spaced multipath channels.**

I. INTRODUCTION

Direct-sequence code division multiple access (DS-CDMA) communication systems have attracted considerable attention as one of the most promising multiplexing technologies for future cellular telecommunications services, such as personal communications, mobile telephony, and indoor wireless networks [1]–[3]. The advantages of DS-CDMA include superior operation in multipath environments, flexibility in the allocation of channels, and increased capacity in fading channels. However, the capacity of DS-CDMA is interference-limited and the ability to remove co-channel interference from other users sharing the same spectrum plays an important factor in the overall system capacity. It has been demonstrated that multiuser detection provides very substantial performance gains over conventional detection schemes [4]–[6]. Most of the multiuser detection schemes proposed in recent years are inherently aimed for uplink [7]–[11]. However, it is obvious that mobile receiver cannot accommodate the same degree of computational complexity.

Adaptive linear receivers based on the linear minimum mean squared error (MMSE) criterion are proposed for the down-link of DS-CDMA systems [12]–[15]. These receivers require only a training sequence of symbols transmitted by the desired user and a coarse knowledge of the timing of the desired user, and can be implemented adaptively using standard algorithms such as least mean squares (LMS) or recursive least squares (RLS) [16]. After the training phase, the receivers can continue to adapt in decision-directed mode, in which symbol decisions made by the receiver are fed back for further adaptation. However, these receivers are vulnerable to sudden channel variations and rapidly fading channels [17]. Therefore, it is necessary to develop blind adaptive mechanisms that do not require knowledge of the symbol sequence of the desired user [18]–[21]. These blind receivers are single-user type receivers with no knowledge beyond that required for implementation of the conventional matched filter detectors for a particular desired user. The blind method in these receivers blindly adapts the linear MMSE receiver based on minimizing the receiver output energy subject to a constraint. In [18] and [21], our blind interference canceller is known as orthogonalizing matched filter (OMF) and we define a constrained minimum mean square (CMMS) criterion to minimize the receiver output energy subject to a constraint of not suppressing the desired user signal energy. The key to an optimal minimization lies in the estimation of a vector, which we define as steering vector. In additive white Gaussian noise (AWGN) environment without any multipath, OMF approaches a blind solution with MMSE performance using a priori assumed steering vector.

In order to exploit multipath diversity, these blind interference cancellers are combined with Rake receivers, such that the multipath combining is carried out after the interference suppression [22]–[24]. Like conventional Rake receivers, blind interference cancellers with Rake are unable to resolve subchip-spaced multipath components [25], [26]. These unresolvable components not only result in suboptimum multipath combining, but also lead to serious performance degradation due to self-cancellation of the desired signal. This can be explained by the fact that these subchip-spaced multipath components become mismatch components [27]. In [28], it is shown that even a small mismatch error can cause a significant performance degradation.

The present contribution overcomes the above limitations by proposing a simple technique to handle subchip-spaced multipath components in blind interference cancellers [29]. This technique termed multiple finger expansion (MFE), involves as-

Manuscript received July 26, 2002; approved for publication by Shigeaki Ogose, Division II Editor, September 8, 2003.

T. Q. S. Quek is with the Department of Electrical Engineering and Computer Science, Massachusetts Institute of Technology, MA 02139, USA, email: qsquek@mit.edu.

H. Suzuki and K. Fukawa are with the Department of Communications and Integrated Systems, Tokyo Institute of Technology, Tokyo, 152-8550, Japan, email: {suzuki, fukawa}@radio.ss.titech.ac.jp.

The material in this paper was presented in part at the IEEE International Symposium on Multi-Dimensional Mobile Communications, Menlo Park, USA, Sept. 1998.

signing subchip-tap spacing in the Rake receiver. This approach is similar to the resolution reduction technique proposed in [30]. By combining MFE with OMF, the new receiver is termed MFE-OMF, and it is able to suppress multipath and multiple access interference blindly as well as to achieve multipath diversity, without any self-cancellation of the desired signal. The structure of MFE is chosen to capture sufficient desired signal energy within the vector space spanned by the fingers of MFE, while reducing any uncaptured desired energy from appearing in the orthogonal vector space generated by MFE-OMF. We will assume that the code tracking circuit is able to track chip-spaced multipath components only and the information is known at the receiver. Although subchip-spaced multipath delays could also be estimated [31], [32], this would greatly increase the computational complexity of MFE-OMF. In this work, we will assume a general structure of MFE without any knowledge of the subchip-spaced multipath delays.

Although the signals at the output of MFE-OMF are correlated, it is still possible to produce diversity gains by using maximal ratio combining (MRC). Nevertheless, improved performance can be obtained by using other optimum combining techniques to whiten the signals at the output of MFE-OMF [33], [34]. However, these techniques are impractical since they are only optimal if the correlation matrix is completely known to the receiver and computational intensive operations are required. In the following, we adopt a suboptimum approach by simply combining the outputs from MFE-OMF using MRC only. The rest of the paper is organized as follows. In Section II, the system model is presented. Our proposed receiver is developed in Section III. In Section IV, our suboptimum multipath combining coupled with detection is discussed. Some computer simulation results are presented in Section V. Finally, Section VI contains the conclusion.

II. SYSTEM MODEL

A complex baseband signal model for DS-CDMA down-link transmission is considered with K users. Without loss of generality, the desired user is assumed to be user number 0. The i-th data symbol for user k, $b_k(i)$, is spread by the spreading waveform $c_k(t)$. Thus, the transmitted signal of user k can be expressed as

$$s_k(t) = \sqrt{E_k} \sum_{i=-\infty}^{\infty} b_k(i) c_k(t - iT),$$

where E_k is the average symbol energy, and T is the symbol interval.

The spreading waveform $c_k(t)$ for the k-th user is shaped with a chip shaping filter $p(t)$ and it can be written as

$$c_k(t) = \sum_{n'=0}^{N_c-1} u_k(n') p(t - n'T_c), \tag{1}$$

where $u_k(n')$ is the spreading signature of the k-th user, and T_c is the chip interval. N_c is the processing gain, such that $N_c = T/T_c$. The chip pulse waveform $p(t)$ is chosen to be the square-root raised cosine pulse with a roll-off factor of α. Without loss of generality, the spreading waveform is normalized so that $\int_{-\infty}^{\infty} |c_k(t)|^2 dt = 1$.

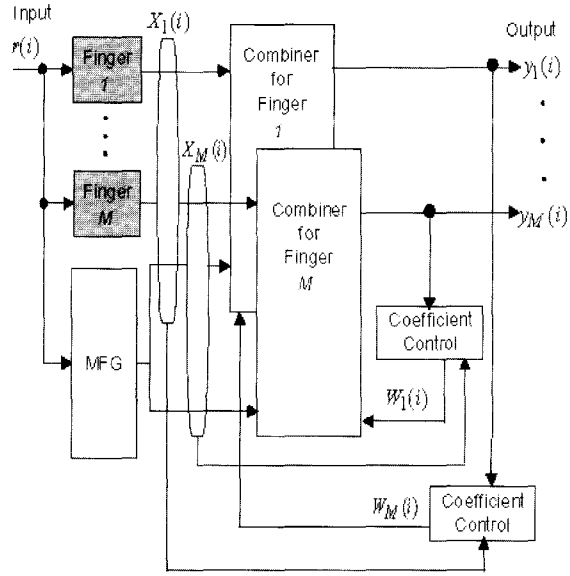

Fig. 1. General structure of MFE-OMF.

The multipath propagation channel from the base station to the mobile station can be characterized by the baseband channel impulse response

$$h(t) = \sum_{d=0}^{D-1} \beta_d(i) \delta(t - \tau_d), \tag{2}$$

where D is the total number of multipaths. $\beta_d(i)$ is the complex channel coefficient of the d-th path when i-th data symbol is transmitted. τ_d is the path delay for the d-th path. The maximum delay spread of the channel model considered is $(D-1)T_c$ and it is known at the receiver.

The received signal can be expressed as

$$r(t) = \sum_{i=-\infty}^{\infty} \sum_{k=0}^{K-1} \sum_{d=0}^{D-1} \beta_d(i) s_k(t - \tau_d) + n(t), \tag{3}$$

where $n(t)$ is a low-pass equivalent of the additive white Gaussian noise with double-sided power spectrum density $N_0/2$.

At the receiver, the received signal in (3) is sampled at a rate of $2/T_c$ and the discrete-time received signal can be expressed as

$$r(iT + j\frac{T_c}{2}) = \sum_{k=0}^{K-1} \sum_{d=0}^{D-1} \sqrt{E_k} \beta_d(i) b_k(i) c_k(j\frac{T_c}{2} - \tau_d) + n(iT + j\frac{T_c}{2}),$$

where the sampling instant is $iT + j\frac{T_c}{2}$ and $0 \le j \le 2N_c - 1$.

III. PROPOSED RECEIVER

A. Structure of MFE-OF

Fig. 1 shows the general structure of MFE-OMF. MFE-OMF consists of a bank of M matched filters matched to each replica

of the desired signal, and an adaptive filter bank to mitigate the MAI associated to all the replicas. The structure of MFE is chosen such that it is able to capture sufficient signal replicas of the desired signal within the vector space spanned by the M fingers. At the same time, it can also reduce any residual energy from the desired signal from appearing in the orthogonal vector space spanned by the adaptive filter bank. The adaptive filter bank is termed as matched filter group (MFG) and it is designed to extract the MAI and noise only.

At MFE, each finger is defined as the spreading waveform of user 0 assigned with a finger delay of Δ_m. The m-th finger of MFE can be expressed as

$$\widetilde{c}_m(t) = \sum_{n'=0}^{N_c-1} u_0(n')p(t-n'T_c-\Delta_{m'}),$$

where

$$\Delta_m = \frac{(m-1)T_c}{(M-1)},$$

for $1 < m \leq M$. Sampling these waveforms at $T_c/2$ gives $\widetilde{\boldsymbol{c}}_m = \left[\widetilde{c}_0^{(m)}, \widetilde{c}_1^{(m)}, \cdots, \widetilde{c}_{2N_c-1}^{(m)}\right]$. In order to generate the impulse response vectors of MFG $\{\widetilde{\boldsymbol{c}}_j\}_{j=M+1}^{2N_c}$, we first assume that these vectors are a set of arbitrary random vectors. By using the Gram-Schmidt orthonormalization, the impulse response vectors of MFE and MFG are regenerated as follows

$$\boldsymbol{a}_l = \frac{\widetilde{\boldsymbol{c}}_l}{\|\widetilde{\boldsymbol{c}}_1\|} \quad \text{for } l = 1,$$

$$\boldsymbol{a}_l = \frac{\widetilde{\boldsymbol{c}}_l - \sum_{i=1}^{l-1}\left(\widetilde{\boldsymbol{c}}_l, \boldsymbol{a}_i\right)\boldsymbol{a}_i}{\left\|\widetilde{\boldsymbol{c}}_l - \sum_{i=1}^{l-1}\left(\widetilde{\boldsymbol{c}}_l, \boldsymbol{a}_i\right)\boldsymbol{a}_i\right\|} \quad \text{for } l > 1,$$

where $\left(\widetilde{\boldsymbol{c}}_l, \boldsymbol{a}_i\right)$ represents the inner product of $\widetilde{\boldsymbol{c}}_l$ and $\boldsymbol{a}_i$. The vectors sets $\{\boldsymbol{a}_l\}_{l=1}^{M}$ and $\{\boldsymbol{a}_l\}_{l=M+1}^{2N_c}$ are the impulse response vectors of MFE and MFG, respectively. With the vector spaces spanned by these orthonormal basis, MFG will only capture MAI and noise.

The output of the l-th filter at the i-th instant can be written as

$$x_l(i) = \sum_{k=0}^{K-1}\sum_{d=0}^{D-1}\sum_{j=0}^{2N_c-1} \beta_d(i)\sqrt{E_k}b_k(i)c_k(j\frac{T_c}{2}-\tau_d)a_l(j) + \tilde{n}_l(i), \quad (4)$$

where $\tilde{n}_l(i)$ is the discrete filtered noise component from the l-th filter. By rearranging the $2N_c \times 1$ vector given by the observations in (4), we can get M sets of $(2N_c - M + 1) \times 1$ vectors. Using vector notation, each $(2N_c - M + 1) \times 1$ vector corresponds to a OMF with respect to m-th finger of MFE and it is given by

$$\boldsymbol{X}_m^H(i) = \left[x_m^*(i), x_{M+1}^*(i), \cdots, x_{2N_c}^*(i)\right], \quad (5)$$

where ^{H} represents Hermitian conjugate and transposition. The output sample from m-th finger is $x_m(i)$ and the MFG output samples are $\{x_l\}_{l=M+1}^{2N_c}$.

Expanding (5) using (4) gives

$$\boldsymbol{X}_m(i) = \boldsymbol{G}_m\boldsymbol{E}\boldsymbol{H}(i)\boldsymbol{b}(i) + \boldsymbol{n}_m(i),$$

with the correlation matrix $\boldsymbol{G}_m$ given by

$$\boldsymbol{G}_m = \begin{bmatrix} \boldsymbol{g}_{1,0} & \cdots & \boldsymbol{g}_{1,K-1} \\ \boldsymbol{g}_{2,0} & \cdots & \boldsymbol{g}_{2,K-1} \\ \vdots & \ddots & \vdots \\ \boldsymbol{g}_{2N_c-M+1,0} & \cdots & \boldsymbol{g}_{2N_c-M+1,K-1} \end{bmatrix},$$

with $\boldsymbol{g}_{q,k} = \left[g_{q,k}^0, \cdots, g_{q,k}^{D-1}\right]$ and $1 \leq q \leq (2N_c - M + 1)$. The element of $\boldsymbol{g}_{q,k}$ can be expressed as

$$g_{q,k}^d = \begin{cases} \sum_{j=0}^{2N_c-1} c_k(j\frac{T_c}{2}-\tau_d)a_m(j) & \text{for } q = 1 \\ \sum_{j=0}^{2N_c-1} c_k(j\frac{T_c}{2}-\tau_d)a_{M+q-1}(j) & \text{for } q > 1. \end{cases}$$

The energy matrix $\boldsymbol{E}$ and the multi-channel coefficient matrix $\boldsymbol{H}(i)$ are given by

$$\boldsymbol{E} = \text{diag}(\boldsymbol{E}_0, \boldsymbol{E}_2, \cdots, \boldsymbol{E}_{K-1}),$$

$$\boldsymbol{H}(i) = \boldsymbol{h}(i)\boldsymbol{I}_K,$$

where $\boldsymbol{E}_k = \sqrt{E_k}\boldsymbol{I}_D$ and $\boldsymbol{h}^H(i) = [\beta_0(i), \cdots, \beta_{D-1}(i)]$. $\boldsymbol{I}_D$ and $\boldsymbol{I}_K$ are defined as $D \times D$ and $K \times K$ identity matrix, respectively. The data sequence vector $\boldsymbol{b}(i)$ is given by

$$\boldsymbol{b}^H(i) = [b_0(i), \cdots, b_{K-1}(i)],$$

and from (4) the noise vector $\boldsymbol{n}_m(i)$ is given by

$$\boldsymbol{n}_m^H(i) = \left[\tilde{n}_m^*(i), \tilde{n}_{M+1}^*(i), \cdots, \tilde{n}_{2N_c}^*(i)\right].$$

The output samples vector $\boldsymbol{X}_m(i)$ in (5) is fed into the combiner for the m-th finger, where the outputs from MFG are adaptively weighted to remove the MAI present in the fingers of MFE by the constrained minimum mean square (CMMS) criterion [18], [21]. The output from m-th combiner $y_m(i)$ is given by

$$y_m(i) = \boldsymbol{W}_m^H\boldsymbol{X}_m(i), \quad (6)$$

where

$$\boldsymbol{W}_m^H = \left[w_{m,0}^*, w_{m,1}^*, \cdots, w_{m,2N_c-M}^*\right].$$

B. CMMS Criterion

The CMMS criterion minimizes the output energy $\langle|y_m(i)|^2\rangle$ under a constraint [18], [21]. This constraint keeps the energy of the desired signal present in the m-th finger constant and prevents self-cancellation of the desired signal in the minimization process. The constraint is defined as

$$\boldsymbol{W}_m^H\boldsymbol{T}_m = 1, \quad (7)$$

where $\boldsymbol{T}_m$ is a $(2N_c - M + 1) \times 1$ vector. The constraint above is somewhat similar to that of the minimum variance distortionless response (MVDR) beamformer [35]. In beamforming, $\boldsymbol{T}_m$

is known as the array propagation vector that contains the information of the angle of arrival of the desired signal. However, in MFE-OMF, $\boldsymbol{T}_m$ is defined as the steering vector and it contains the information of the distribution of the desired signal energy in the output samples vector in (5).

The cost function $J^{(m)}$ is defined by

$$\begin{aligned} J^{(m)} &= \langle |\boldsymbol{W}_m^H \boldsymbol{X}_m(i)|^2 \rangle + \lambda_m (\boldsymbol{W}_m^H \boldsymbol{T}_m - 1) \\ &= \boldsymbol{W}_m^H \boldsymbol{R}_m \boldsymbol{W}_m + \lambda_m (\boldsymbol{W}_m^H \boldsymbol{T}_m - 1), \end{aligned}$$

where $\boldsymbol{R}_m = \langle \boldsymbol{X}_m(i) \boldsymbol{X}_m^H(i) \rangle$ and λ_m is a Lagrange multiple. By solving $\delta J^{(m)} / \delta \boldsymbol{W}_m = \boldsymbol{0}$ subject to the constraint defined in (7), the solution $\widetilde{\boldsymbol{W}}_m$ is

$$\widetilde{\boldsymbol{W}}_m^H = -\lambda_m \boldsymbol{R}_m^{-1} \boldsymbol{T}_m, \tag{8}$$

$$\lambda_m = \left(\boldsymbol{T}_m^H \boldsymbol{R}_m^{-1} \boldsymbol{T}_m \right)^{-1},$$

and its minimum energy $J_{\min}^{(m)}$ becomes

$$J_{\min}^{(m)} = \widetilde{\boldsymbol{W}}_m^H \boldsymbol{R}_m^{-1} \widetilde{\boldsymbol{W}}_m = \left(\boldsymbol{T}_m^H \boldsymbol{R}_m^{-1} \boldsymbol{T}_m \right)^{-1}.$$

On the other hand, the optimum Wiener solution $\boldsymbol{W}_{\text{opt}}^{(m)}$ is given by

$$\boldsymbol{W}_{\text{opt}}^{(m)} = \boldsymbol{R}_m^{-1} \boldsymbol{V}_m, \tag{9}$$

where $\boldsymbol{V}_m = \langle \boldsymbol{X}_m(i) z_0^*(i) \rangle$ represents the crosscorrelation between $\boldsymbol{X}_m(i)$ and the desired signal component $z_0(i)$ in $\boldsymbol{X}_m(i)$. $z_0(i)$ is purely the product of the transmitted desired data symbol $b_0(i)$ and the channel impulse response in (2). This is a time varying component and is unknown *a priori*.

In order for $\widetilde{\boldsymbol{W}}_m = \boldsymbol{W}_{\text{opt}}^{(m)}$, $\boldsymbol{T}_m$ has to satisfy the relationship $\boldsymbol{T}_m = \kappa \boldsymbol{V}_m$ where κ is any nonzero complex constant. However, $\boldsymbol{V}_m$ is unknown *a priori*. Therefore, a blind optimization with an approximated $\boldsymbol{T}_m$ can be implemented in MFE-OMF as follows

$$\boldsymbol{T}_m = \boldsymbol{T} = [1 \;\; 0 \;\; \cdots \;\; 0] \quad \text{for } 1 \le m \le M.$$

Based on this approximation, the solution in (8) will converge to the optimum Wiener solution in (9) as long as no desired signal exists in MFG.

C. Adaptive Algorithm

The adaptive algorithm employed here is the Recursive Least Squares (RLS) algorithm subject to the constraint in (7). Hence, we termed this algorithm as Constrained Recursive Least Squares (CRLS) algorithm. The main reason for choosing RLS algorithm rather than LMS algorithm is that the convergence rate of the RLS algorithm is typically an order of magnitude faster rather than that of the LMS algorithm [18], [21]. The recursive equations to update the combining coefficients vector $\boldsymbol{W}_m$ are

$$\begin{aligned} \boldsymbol{P}_m(i) &= \lambda^{-1} \boldsymbol{P}_m(i-1) \\ &\quad - \frac{(\lambda^{-1})^2 \boldsymbol{P}_m(i-1) \boldsymbol{X}_m(i) \boldsymbol{X}_m^H(i) \boldsymbol{P}_m(i-1)}{1 + \lambda^{-1} \boldsymbol{X}_m^H(i) \boldsymbol{P}_m(i-1) \boldsymbol{X}_m(i)}, \end{aligned}$$

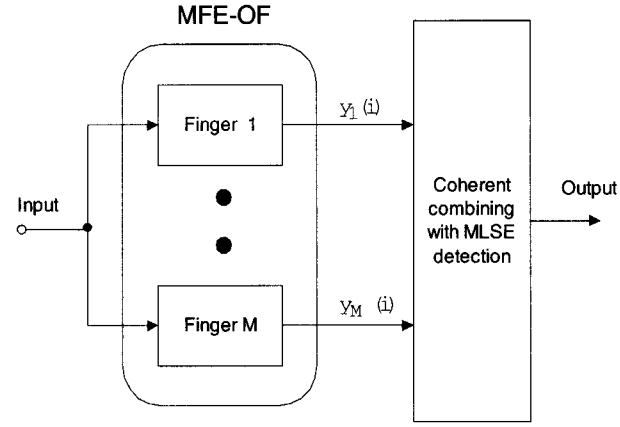

Fig. 2. Suboptimum diversity combining with detection.

$$\begin{aligned} \boldsymbol{W}_m(i) &= \frac{\boldsymbol{P}_m(i) \boldsymbol{T}_m}{\boldsymbol{T}_m^H \boldsymbol{P}_m(i) \boldsymbol{T}_m}, \\ y_m(i) &= \boldsymbol{W}_m(i-1) \boldsymbol{X}_m(i), \end{aligned}$$

where $\boldsymbol{P}_m(i) = \boldsymbol{R}_m^{-1}(i)$ and λ is the forgetting factor. The derivation above utilized the relationship as shown below

$$\begin{aligned} \boldsymbol{R}_m(i) &= \sum_{k=1}^{i} \lambda^{i-k} \boldsymbol{X}_m(k) \boldsymbol{X}_m^H(k) \\ &= \lambda \boldsymbol{R}_m(i-1) + \boldsymbol{X}_m(i) \boldsymbol{X}_m^H(i), \end{aligned}$$

and in order to initialize the algorithm, the below values are set

$$\begin{aligned} \boldsymbol{P}_m(0) &= \delta^{-1} \boldsymbol{I}, \\ \boldsymbol{W}_m(0) &= \frac{\boldsymbol{T}_m}{\boldsymbol{T}_m^H \boldsymbol{T}_m}, \end{aligned}$$

where δ is a small positive constant.

IV. SUBOPTIMUM DIVERSITY DETECTION

The diversity receiver structure collects the useful signal energy after interference suppression from each finger in (6) and then suboptimally combines the collected energies to make a final decision on the received data symbol. Fig. 2 shows the block diagram of the suboptimum diversity combining with detection. Since the receiver is only blind in terms of interference cancellation, we still need to combine each of the suppressed multipath components together for data detection. In general, we can employ either non-coherent combining or coherent combining. In the former, it is used with differential detection and the non-coherent combining can be expressed as $\sum_{m=1}^{M} y_m^*(i-1) y_m(i)$. In the latter, the coherent combining requires some state information to perform data detection. In our paper, we have employed the latter and our combining algorithm is based on the coherent detection with predictive carrier recovery using Maximum Likelihood Sequence Estimation (MLSE) [36]. Due to the high correlation between adjacent samples, we have used MLSE and the whole transmitted sequence has been taken into account in order to minimize the probability of error.

Unlike the non-coherent combining mentioned above, our combining algorithm will require preamble and postamble symbols for both channel estimation and MLSE sequence detection.

In the above communication system, we consider the transmission of $\mathcal{A}_{\mathcal{I}} = 2^{\mathcal{I}}$ possible data sequences. According to the maximum likelihood (ML) decision rule, the likelihood function of the observation $\boldsymbol{y}$, conditioned on l-th transmitted information hypotheses, $\boldsymbol{b}_0^{(l)}$ is to be maximized

$$p(\boldsymbol{y}|\widehat{\boldsymbol{b}}_0) = \max_{l \in \mathcal{A}_{\mathcal{I}}} p(\boldsymbol{y}|\boldsymbol{b}_0^{(l)}),$$

such that $\widehat{\boldsymbol{b}}_0 = [\widehat{b}_0(1), \cdots, \widehat{b}_0(\mathcal{I})]^{\mathcal{H}}$ is the most likely transmitted data sequence of the desired user. In a communication link with M path diversity, the likelihood function becomes

$$p(\boldsymbol{y}_1, \cdots, \boldsymbol{y}_M|\boldsymbol{b}_0^{(l)}) = \prod_{m=1}^{M} p(\boldsymbol{y}_m|\boldsymbol{b}_0^{(l)}).$$

The above function is valid if there is no correlation between $\{y_1(i), \cdots, y_M(i)\}$. Since we know that the outputs from MFE-OMF are correlated, we will obtain a suboptimum combining performance using the above function.

Let $\xi(l,i) \equiv \{y_m(1), \cdots, y_m(i), \boldsymbol{b}_0^{(l)}\}$ represent the observation up to time i and hypotheses l. By repeated application of the definition of a conditional pdf to $p(\boldsymbol{y}_m|\boldsymbol{b}_0^{(l)})$, the following is obtained [37]

$$p(\boldsymbol{y}_m|\boldsymbol{b}_0^{(l)}) = \prod_{i=1}^{\mathcal{I}} p\big(y_m(i)|\xi(l,i-1)\big). \tag{10}$$

The term $p\big(y_m(i)|\xi(l,i-1)\big)$ is the pdf pertaining to the one-step prediction of the received sample $y_m(i)$, given the past received signal sequence $\{y_m(1), \cdots, y_m(i-1)\}$ and the information hypothesis $\boldsymbol{b}_0^{(l)}$ up to the present. By assuming that $\boldsymbol{y}_m(i)$ is a complex Gaussian distributed i.i.d. random variable, we can also assume that $p\big(y_m(i)|\xi(l,i-1)\big)$ is Gaussian distributed with conditional mean $\widehat{y}_m(l,i)$ and variance $\sigma_{y,m}^2(i)$, given by

$$p\big(y_m(i)|\xi(l,i-1)\big) = \frac{1}{\pi\sigma_{y,m}^2(i)} \exp\left(-\frac{|y_m(i) - \widehat{y}_m(l,i)|^2}{\sigma_{y,m}^2(i)}\right).$$

With the assumption that the data sequence $\boldsymbol{b}_0^{(l)}$ has been transmitted, the mean $\widehat{y}_m(l,i)$ can be expressed as

$$\widehat{y}_m(l,i) = E\left[y_m(i)|\xi(l,i-1)\right] = b_0^{*(l)}(i) \underbrace{E\left[h_m(i)|\xi(l,i-1)\right]}_{\widehat{h}_m(l,i)},$$

where $\widehat{h}_m(l,i)$ is the optimal linear prediction estimate of $h_m(i)$. The estimate may be obtained by using the estimator equation of an $\mathcal{I}$-th order linear prediction as follows [16]:

$$\widehat{h}_m(l,i) = \sum_{j=1}^{\mathcal{I}} f_j(i)\widehat{b}_0^{*(l)}(i-j)y_m(i-j),$$

where $f_j(i)$ are the filter weights. Note that $\widehat{h}_m(l,i)$ is data dependent and needs to be calculated for every possible hypotheses. The filter weights $\{f_j(i)\}$ can be pre-computed and used for all l hypotheses. In a stationary or slowly fading channel $\{f_j(i)\}$ can be truncated by a time independent linear prediction filter of order N_{av}, such that $f_j = N_{\text{av}}^{-1}$. The channel estimate $\widehat{h}_m(l,i)$ then becomes

$$\widehat{h}_m(l,i) = \sum_{j=1}^{N_{\text{av}}} N_{\text{av}}^{-1}\widehat{b}_0^{*(l)}(i-j)y_m(i-j). \tag{11}$$

Note that the variance $\sigma_{y,m}^2$ is not data dependent. Taking the logarithm in (10), the decision metric becomes

$$\Lambda(l,\mathcal{I}) = \sum_{i=1}^{\mathcal{I}} \sum_{m'=1}^{M} \left|b_0^{*(l)}(i)y_m(i) - \widehat{h}_m(l,i)\right|^2,$$

where the factors which are constant and independent of l have been removed. Minimizing $\Lambda(l,\mathcal{I})$ over all possible hypotheses l is equivalent to the ML decision rule

$$\Lambda_{\min} = \min_{l \in \mathcal{A}_{\mathcal{I}}}(l,\mathcal{I}),$$

where the MLSE approach minimizes the Euclidean distance between $y_m(i)$ and the channel estimate in respect to all possible hypotheses l of the transmitted data sequence. The prohibitive high complexity of the MLSE detection due to the exponential growth of $\mathcal{A}_{\mathcal{I}}$ can be reduced by employing the Viterbi algorithm. This is equivalent to the case of equalization of channels with inter-symbol interference by MLSE detection [37].

Let $\Lambda_s(i)$ denote the survivor path up to sample i at a particular state, that is the metric with the minimum distance entering at this state is defined as

$$\Lambda_s(i) = \min_{l \in \widetilde{\mathcal{A}}_i}\{\Lambda(l,i)\},$$

where $\widetilde{\mathcal{A}}_i$ is the number of hypotheses entering this state up to sample i. Consider that this survivor path extends to sample $i+1$, we compute the metric to the next possible state

$$\Lambda(l,i+1) = \Lambda_s(i) + \sum_{m=1}^{M} \left|b_0^{*(l)}(i+1)y_m(i+1) - \widehat{h}_m(l,i+1)\right|^2.$$

At each state, there are two branches entering it , such that the one with the larger metric is discarded, leaving one survivor path per state. After a delay of $\mathcal{I}$ symbols, only one survivor path exists, which yields the estimated desired data sequence $\widehat{\boldsymbol{b}}_0$. Hence, we are able to coherently combine the outputs from MFE-OMF in a suboptimum manner. Although this suboptimum method suffers a performance loss due to the correlation between the outputs from MFE-OMF, it is simpler and practical compared to other optimum techniques [33], [34].

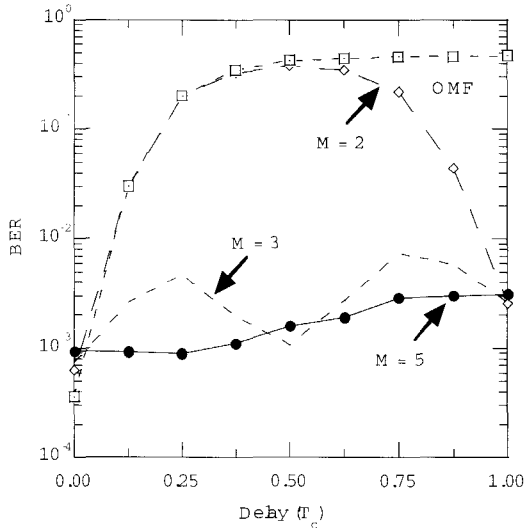

Fig. 3. BER versus τ_1 in the static environment.

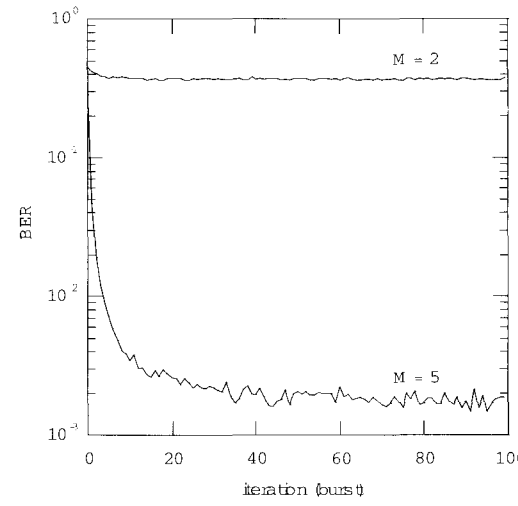

Fig. 4. Convergence characteristics of MFE-OMF in static environment.

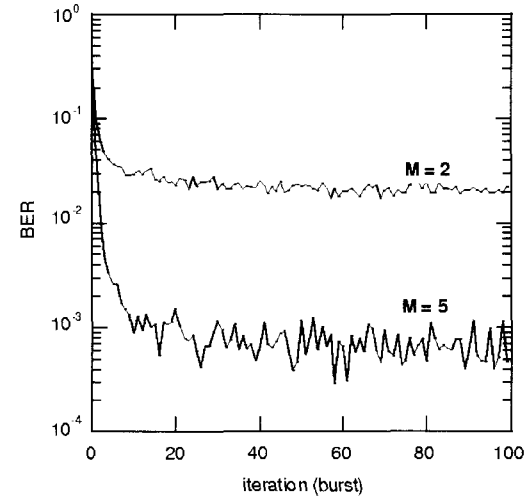

Fig. 5. Convergence characteristics of MFE-OMF in fading environment.

V. SIMULATION RESULTS

A. Simulation Conditions

We examine a bit rate of 10 kbps DS-CDMA system with $N_c = 16$. The roll-off factor α of $p(t)$ in (1) is 1.0. The mutual correlation of users' spreading signatures used is less than 0.25 [21]. Perfect down-link power control is assumed to maintain equal average receiving power from respective users. The burst sequence is made up of 64 data symbols and 5 preamble and postamble symbols respectively. The preamble and postamble symbols are used to determine the initial and final states for coherently detecting the burst sequence by using MLSE. The order of the linear prediction filter N_{av} used in (11) is 4.

Our channel model is based on the uniform profile with two paths, one direct path and one delay path with delay τ_1. Although modeling the path delay τ_1 as independently random variable may reflect more accurately the practical situation, fixed path delay τ_1 leads to a tractable analysis which accurately reflects the quantitative effects of the timing errors in our proposed receiver. For simplicity, the maximum delay spread considered is T_c and it is known at the receiver. In the static environment, the path gains of the two multipath components are fixed at $1/\sqrt{D}$ and the two paths are mutually $\pi/2$ out of phase. These parameters are particularly designed to verify the effectiveness of MFE-OMF under severe condition in static environment. Whereas in the frequency selective fading environment, the two multipath components undergo independent Rayleigh fading. Simulations are allowed to run long enough for the tap weights to converge before errors are counted.

B. Propagation Delay Performance

We first illustrate the BER performance of MFE-OMF with $M = 2, 3, 5$ in static environment versus propagation delay in Fig. 3. The number of active users is K = 8 and E_b/N_0 = 8 dB. The performance of OMF [21] is extremely poor with the BER range remaining above 10^{-2} for $\tau_1 = 0.125\ T_c$ and above. Hence, we can see that OMF is very sensitive to mismatch problem. When M = 2, MFE-OMF operates well at $\tau_1 = 0$ and $1.0\ T_c$ and degrades very much at $0.5\ T_c$, whereas for M = 3, it degrades at $\tau_1 = 0.25$ and $0.75\ T_c$. These performance degradation is due to the self-cancellation problem when MFE is unable to fully capture the desired signal replicas, resulting in the appearance of residual desired signal energy in MFG. However, for M = 5, MFE-OMF operates well over the whole delay spread from $\tau_1 = 0$ to $1.0\ T_c$. This shows the effectiveness of increasing the number of subchip-spaced fingers. In addition, the performance of MFE-OMF is still acceptable despite of the suboptimum diversity combining.

C. Convergence Characteristics

Fig. 4 shows the initial convergence characteristics of MFE-OMF in static environment. The number of active users is K = 8 with $\tau_1 = 0.5\ T_c$ assigned to each user and E_b/N_0 is 8 dB. The performance measure plotted here is the BER versus number of iteration (burst). In static environment, the performance of M = 2 is extremely poor with BER remaining above 10^{-1} since the residual desired signal appears in MFG. M = 5 converges well as expected since MFE sufficiently captures the energies of the

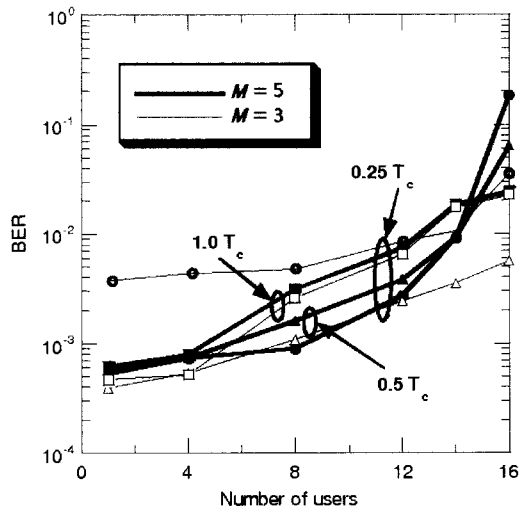

Fig. 6. User capacity of MFE-OMF.

desired signal replicas.

On the other hand, Fig. 5 shows the initial convergence characteristics of MFE-OMF in frequency selective fading environment. The number of active users is $K = 8$ with $\tau_1 = 0.5\ T_c$ assigned to each user and E_b/N_0 is 20 dB. The maximum doppler frequency is 40 Hz and the performance measure is similar to that in Fig. 4. The BER of $M = 2$ remains above 10^{-2} and it can be seen that the MFE-OMF does not degrade as badly as in the static environment even with the same number of fingers. This is because the multipath components fade independently in the frequency selective fading channels. In frequency selective fading environment, each multipath component of the desired user corresponds to its own distinct eigenvector [27]. Hence, the appearance of the residual desired signal in MFG does not affect the performance as badly as in the static condition.

D. User Capacity

We next consider the user capacity of MFE-OMF in static environment for $M = 3$ and 5. $\tau_1 = 0.25$, 0.5, and 1.0 T_c are assigned to each user k in three different simulations. The performance measure is the BER versus number of active users and it is plotted in Fig. 6. While $M = 3$ is seen to be better than $M = 5$ at $\tau_1 = 0.5$ and 1.0 T_c, it is still limited by the unexpanded residual desired signal that appears in MFG, which leads to performance degradation in other delay time τ_1. At $\tau_1 = 0.25\ T_c$, $M = 5$ outperforms $M = 3$ up to 14 users. If the acceptable BER is 10^{-3}, then about 5 users can be supported with $M = 5$ with E_b/N_0 of 8 dB. However, if the acceptable BER is 10^{-2}, then both $M = 5$ and $M = 3$ can support about 13 users.

E. BER Performance

The performance of MFE-OMF in static environment is studied with $K = 8$ and $\tau_1 = 0.25\ T_c$ for each user. The simulated BER performance is plotted in Fig. 7. $M = 2$ performs poorly due to mismatch problem. At low E_b/N_0, $M = 3$ and $M = 5$ have almost similar performance. However, as E_b/N_0 increases, the BER performance of $M = 3$ degrades compared to

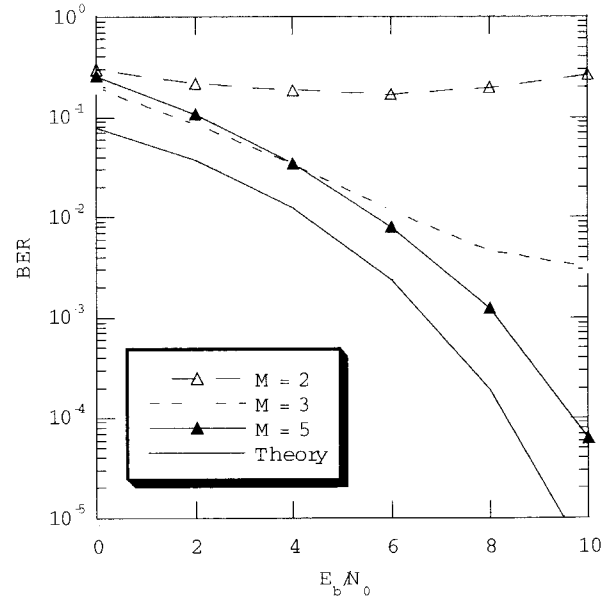

Fig. 7. BER versus E_b/N_0 in the static environment.

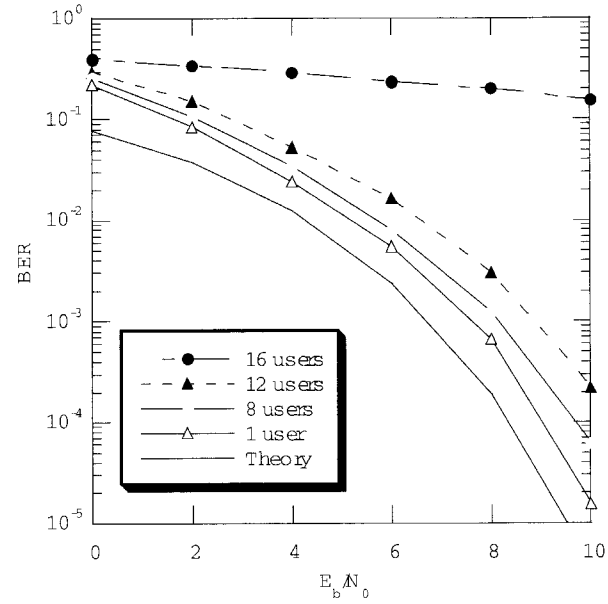

Fig. 8. BER performance of 5 Finger MFE-OMF.

$M = 5$. This is because as E_b/N_0 increases, the residual desired energy that appears in MFG gets stronger and self-cancellation becomes significant. In addition, under the same conditions as in Fig. 7, the BER performance of 5 Finger MFE-OMF with different system capacity is plotted in Fig. 8. The number of active users is $K = 1$, 8, 12 ,and 16. It can be observed that in the single user case, the BER performance of $M = 5$ degrades about 1 dB compared to the single-user theoretical BER for BPSK coherent detection. As the number of users increases, the BER performance of $M = 5$ is degraded by the increase in MAI. When the allowable BER is less than 10^{-2}, $M = 5$ can support 12 users, which corresponds to 0.75 times the processing gain of 16, with a degradation of 1.5 dB.

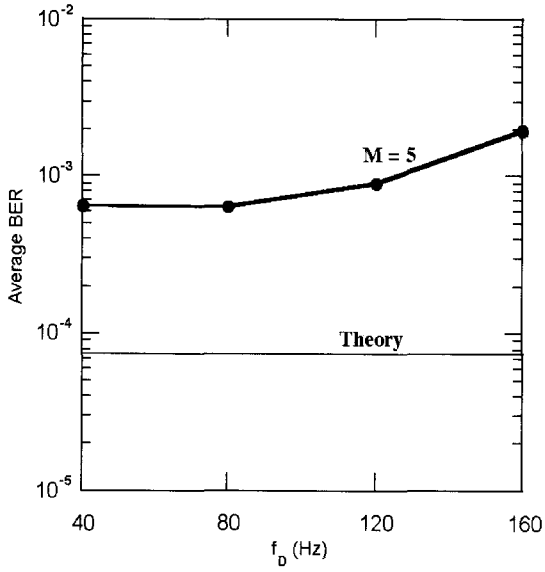

Fig. 9. Fading performance of 5 finger MFE-OMF.

F. Fading Performance

In Fig. 9, the BER performance of 5 Finger MFE-OF versus maximum Doppler frequency f_D for $K = 8$, $E_b/N_0 = 20$ dB, and $\tau_1 = 0.5\ T_c$ is shown. The theoretical average BER per branch, $P_e = 3/4(E_b/N_0)^2$, for a 2 branch diversity with maximal ratio combining is plotted for comparison. We can see that the MFE-OMF with suboptimum diversity combining performs worse than the theoretical bound. This gap can be narrowed by using optimum techniques in [33] and [34] at the expense of additional computational complexity. It can also be seen that as f_D increases the average BER becomes larger. This can be explained by the fact that, at slow fading, a deep fade is likely to last longer and the performance of the linear prediction filter is better for large N_{av}. On the other hand, the linear prediction filter is unable to track the fading distortion with large N_{av} as f_D becomes larger. This problem can be solved by employing a higher-order state variable model to model the rapidly varying fading channels and uses a Kalman filter to track the fading channels [38], [39].

VI. CONCLUSIONS

In this paper, we considered the problem of blind interference canceller in the presence of subchip-spaced multipath channels for the DS-CDMA down-link. The performance of our proposed receiver was extensively simulated under different conditions. Computer simulations verify the effectiveness of our proposed receiver to handle subchip-spaced multipath components and still suppresses the MAI significantly. Based on the results, the mismatch problem in OMF is more severe in static environment than in the fading environment. This can be explained by the fact that each multipath component corresponds to its own distinct eigenvector in frequency selective fading channels and self-cancellation is greatly minimized. Lastly, despite that the diversity combining in MFE-OMF is suboptimum, the performance is still acceptable.

REFERENCES

[1] R. Kohno, R. Median, and L. B. Milstein, "Spread spectrum access method for wireless communications," *IEEE Commun. Mag.*, pp. 58–67, Jan. 1995.

[2] T. Ojanpera and R. Prasad, *Wideband CDMA for third generation mobile communications*, Artech House, 1998.

[3] F. Adachi, M. Sawahashi, and H. Suda, "Wideband DS-CDMA for next-generation mobile communication systems," *IEEE Commun. Mag.*, pp. 56–69, Sept. 1998.

[4] A. Duel-Hallen, J. Holtzman, and Z. Zvonar, "Multiuser detection for CDMA systems," *IEEE Pers. Commun. Mag.*, pp. 46–58, Apr. 1995.

[5] S. Moshavi, "Multiuser detection for DS-CDMA communications," *IEEE Commun. Mag.*, pp. 12–36, Oct. 1996.

[6] S. Verdu, *Multiuser Detection*, Cambridge Univ. Press, 1998.

[7] S. Verdu, "Minimum probability of error for asynchronous Gaussian multiple-access channels," *IEEE Trans. Inform. Theory*, vol. 32, pp. 85–96, Jan. 1986.

[8] R. Lupas and S. Verdu, "Near-far resistance of multiuser detectors in asynchronous channels," *IEEE Trans. Commun.*, vol. 38, pp. 496–508, Apr. 1990.

[9] M. K. Varanasi and B. Aazhang, "Near-optimum detection in synchronous code-division multiple-access communications," *IEEE Trans. Commun.*, vol. 39, pp. 725–736, May 1991.

[10] P. Patel and J. Holtzman, "Analysis of a simple successive interference cancellation scheme in a DS/CDMA system," *IEEE J. Select. Areas Commun.*, vol. 12, pp. 796–807, June 1994.

[11] A. Duel-Hallen, "Decorrelating decision-feedback multiuser detector for synchronous code-division multiple-access channel," *IEEE Trans. Commun.*, vol. 41, pp. 285–290, Feb. 1993.

[12] U. Madhow and M. L. Honig, "MMSE interference suppression for direct-sequence spread-spectrum CDMA," *IEEE Trans. Commun.*, vol. 42, pp. 3178–3188, Dec. 1994.

[13] S. L. Miller, "An adaptive direct-sequence code-division multiple-access receiver for multiuser interference rejection," *IEEE Trans. Commun.*, vol. 43, pp. 1746–1755, Feb./Mar./Apr. 1995.

[14] P. B. Rapajic and B. S. Vucetic, "Adaptive receiver structures for asynchronous CDMA systems," *IEEE J. Select. Areas Commun.*, vol. 12, pp. 685–697, May 1994.

[15] A. Klein, "Data detection algorithms specially designed for the downlink of CDMA mobile radio systems," in *Proc. IEEE VTC'97*, May 1997, pp. 203–207.

[16] S. Haykin, *Adaptive Filter Theory*, 3rd. Edt., Prentice-Hall, 1998.

[17] U. Madhow, "Blind adaptive interference suppression for direct-sequence CDMA," *Proc. IEEE*, vol. 86, pp. 2049–2069, Oct. 1998.

[18] K. Fukawa and H. Suzuki, "Orthogonalizing Matched Filter (OMF) detection for DS-CDMA mobile radio systems," in *Proc. GLOBECOM'94*, Nov. 1994, pp. 385–389.

[19] M. Honig, U. Madhow, and S. Verdu, "Blind adaptive multiuser detection," *IEEE Trans. Inform. Theory*, vol. 41, pp. 944–960, July 1995.

[20] M. K. Tsatsanis, "Inverse filtering criteria for CDMA systems," *IEEE Trans. Signal Processing*, vol. 45, pp. 102–112, Jan. 1997.

[21] K. Fukawa and H. Suzuki, "Orthogonalizing Matched Filter (OMF) detection for DS-CDMA mobile communication systems," *IEEE Trans. Veh. Technol.*, vol. 48, pp. 188–197, Jan. 1999.

[22] K. Fukawa and H. Suzuki, "BER performance of Orthogonalizing Matched Filter (OMF) in mobile DS-CDMA systems," in *Proc. ICUPC'95*, Nov. 1995, pp. 42–46.

[23] H. Liu and K. Li, "A decorrelating RAKE receiver for CDMA communications over frequency-selective fading channels," *IEEE Trans. Commun.*, vol. 47, pp. 1036–1045, July 1999.

[24] G. E. Bottomley, T. Ottosson, and Y.-P. E. Wang, "A gneralized RAKE receiver for interference suppression," *IEEE J. Select. Areas Commun.*, vol. 18, pp. 1536–1545, Aug. 2000.

[25] B. W. Hart, R. D. J. V. Nee, and R. Prasad, "Performance degradation due to code tracking errors in spread-spectrum code-division multiple-access system," *IEEE J. Select. Areas Commun.*, vol. 14, pp. 1669–1679, Oct. 1996.

[26] R. de Gaudenzi, "Direct-sequence spread-spectrum chip tracking in the presence of unresolvable multipath components," *IEEE Trans. Veh. Technol.*, vol. 48, pp. 1573–1583, Sept. 1999.

[27] H. Suzuki and K. Fukawa, "A linear interference canceller with a blind algorithm for CDMA mobile communication systems," in *Proc. IEEE VTC'97*, May 1997, pp. 208–212.

[28] P. Orten and T. Ottosson, "Robustness of DS-CDMA multiuser detectors," in *Proc. GLOBECOM'97*, Nov. 1997, pp. 144–148.

[29] Q. S. Quek, H. Suzuki, and K. Fukawa, "Adaptive optimal filter with multiple finger expansion for CDMA mobile communications," in *Proc. IEEE*

3rd Int. Symp. Multi-Dimensional Mobile Commun., Sept. 1998, pp. 156–160.

[30] J. Yang, "Diversity receiver scheme and system performance evaluation for a CDMA system," *IEEE Trans. Commun.*, vol. 47, pp. 272–280, Feb. 1999.

[31] R. Vaughan and N. Scott, "Super-resolution of pulsed multipath channels for delay spread characterization," *IEEE Trans. Commun.*, vol. 47, pp. 343–347, Mar. 1999.

[32] Z. Kostic and G. Pavlovic, "Resolving subchip-spaced multipath components in CDMA communication systems," *IEEE Trans. Veh. Technol.*, vol. 48, pp. 1803–1808, Nov. 1999.

[33] K. J. Kim *et al.*, "Effect of tap-spacing on the performance of direct-sequence spread-spectrum RAKE receiver," *IEEE Trans. Commun.*, vol. 48, pp. 1029–1036, June 2000.

[34] M. R. Hueda, G. Corral-Briones, and C. E. Rodriguez, "MMSEC-RAKE receivers with resolution reduction of the diversity branches: Analysis, simulation, and applications," *IEEE Trans. Commun.*, vol. 49, pp. 1073–1081, June 2001.

[35] D. H. Johnson and D. E. Dudgeon, *Array Signal Processing: Concepts and Techniques*, Prentice-Hall, 1993.

[36] K. Fukawa and H. Suzuki, "Coherent detection with predictive channel estimation - application of RLS-MLSE to coherent detection for mobile radio communications," *Technical Report IEICE*, RCS-92-93, Nov. 1992.

[37] M. L. Moher and J. H. Lodge, "Maximum likelihood sequence estimation of CMP signals transmitted over Rayleigh flat fading channels," *IEEE Trans. Commun.*, vol. 38, pp. 787–794, June 1990.

[38] H. Suzuki, "Adaptive signal processing for optimal transmission in mobile radio communications," *IEICE Trans. Commun.*, vol. E77-B, pp. 535–544, May 1994.

[39] R. Haeb and H. Meyr, "A systematic approach to carrier recovery and detection of digitally phase modulated signals on fading channels," *IEEE Trans. Commun.*, vol. 37, pp. 748–754, July 1989.

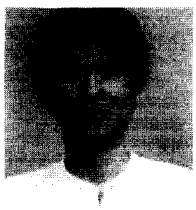

Tony Q.S. Quek was born in Singapore. He received the B.E. and M.E. degrees in electrical and electronics engineering from Tokyo Institute of Technology, Tokyo, Japan, in 1998 and 2000, respectively. From 2001 to 2002, he was with Centre for Wireless Communications, National University of Singapore (now Institute for Infocomm Research) as a research engineer. Presently, he is pursuing his Ph.D. degree in the department of electrical engineering and computer science at Massachusetts Institute of Technology, Massachusetts, U.S.A. His research interests include ultra-wideband communications, sensor networks, and information-theoretic study of wireless systems. He is a student member of IEEE.

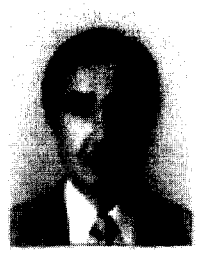

Hiroshi Suzuki received the B.S. degree in Electrical Engineering, the M.S. degree in Physical Electronics, and the Dr. Eng. degree in Electrical and Electronics Engineering, all from the Tokyo Institute of Technology, Tokyo, Japan, in 1972, 1974, and 1986, respectively. He joined the Electrical Communication Laboratories, Nippon Telegraph and Telephone Corporation (NTT), Japan, in 1974. He was engaged in research on devices in millimeter wave regions. Since 1978, he has been engaged in fundamental and developmental researches on digital mobile communication systems. He was an Executive Research Engineer in the Research and Development Department, NTT Mobile Communications Network, Inc. (NTT DoCoMo) from 1992 to 1996. Since September 1996, he has been Professor at the Tokyo Institute of Technology. He is currently interested in various applications of the adaptive signal processing to radio signaling: adaptive array, multiuser detection, and interference canceling for future advanced multiple-access communication systems. Dr. Suzuki is a Member of IEEE since 1978. He is also a Member of the Institute of Electronics, Information, and Communication Engineers (IEICE) of Japan. He received Paper Award from IEICE in 1995. He was the Chairman of the Radio Communication Systems (RCS) Technical Group in the Communications Society of IEICE from 1999 to 2001.

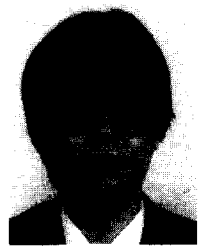

Kazuhiko Fukawa received the B.S. and M.S. degrees in physics, and the Dr. Eng. degree in electrical and electronics engineering, all from Tokyo Institute of Technology, Tokyo, Japan, in 1985, 1987, and 1999 respectively. He joined NTT, Japan, in 1987. Since then, he has been engaged in research on digital mobile radio communication systems and applications of the adaptive signal processing, including adaptive equalization, interference cancellation, and adaptive arrays. He was a Senior Research Engineer at NTT Mobile Communications Network Inc., from 1994 to 2000. Since April 2000, he has been an Associate Professor at the Tokyo Institute of Technology. Dr. Fukawa is a member of IEEE and the Institute of Electronics, Information and Communication Engineers (IEICE) of Japan.